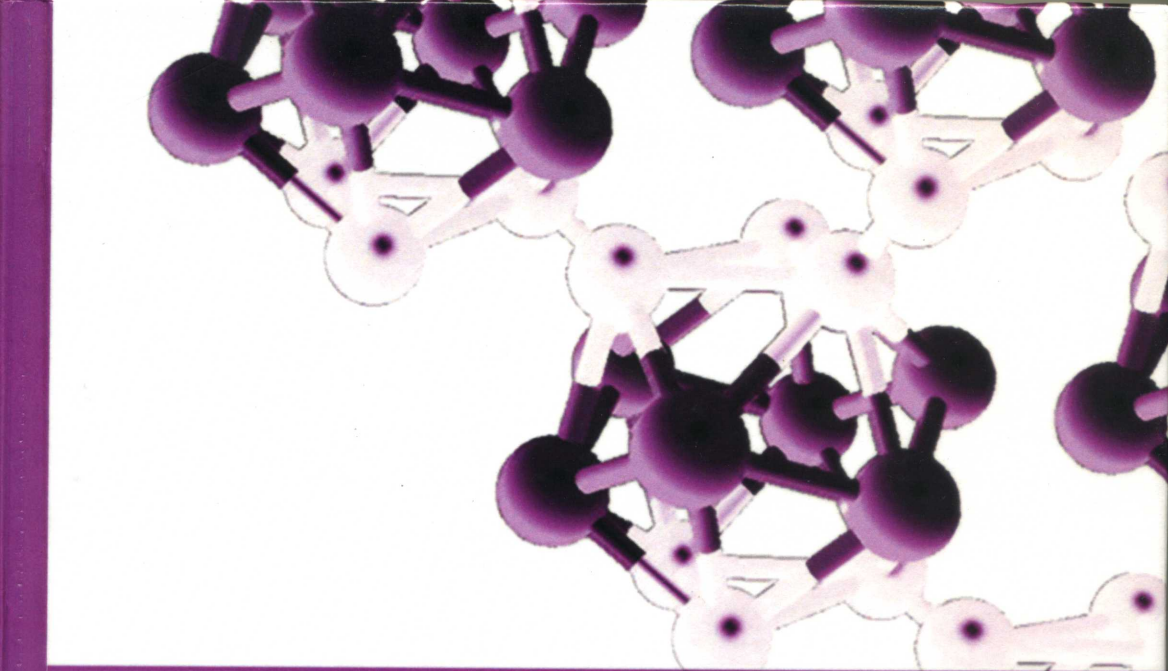

edited by Junji Haruyama

CARBON-BASED SUPERCONDUCTORS

Toward High-T_c Superconductivity

CARBON-BASED SUPERCONDUCTORS

Toward High-T_c Superconductivity

edited by
Junji Haruyama

PAN STANFORD PUBLISHING

Published by

Pan Stanford Publishing Pte. Ltd.
Penthouse Level, Suntec Tower 3
8 Temasek Boulevard
Singapore 038988

Email: editorial@panstanford.com
Web: www.panstanford.com

British Library Cataloguing-in-Publication Data
A catalogue record for this book is available from the British Library.

Carbon-Based Superconductors: Toward High-T_c Superconductivity

ISBN 978-981-4303-30-9 (Hardcover)
ISBN 978-981-4303-31-6 (eBook)

Printed in the USA

Contents

Foreword

I was personally drawn into the study of graphite intercalation compounds because of the findings of superconductivity in KC_8 at Bell Labs. I pursued research in the field of graphene intercalation compounds for a 15-year period starting in 1973. It was known in 1947 that a single layer of graphene was unusual in having a linear $E(k)$ dispersion relation, whereas other materials studied prior to 1960 had quadratic carrier dispersion relations. This indicated that single-layer and few-layer sp^2 carbon materials based on graphene would have other electronic properties different from conventional semiconducting materials. My own background, when I started the study of carbon-based materials, was in superconductivity, and for this reason I have been interested in the possibility of superconductivity existing in carbon materials. Consequently, in the 1960s, we did some preliminary magneto-optic studies on superconducting KC_8 as suggested by Ted Geballe, an author on the 1965 paper by the Bell Labs group on superconducting KC_8. Added interest to the field was provided by the strong statements made by Bernt Matthias starting in the 1950s to the effect that magnetism and superconductivity could not coexist. Matthias was an early pioneer in the development of many new type II superconductors and became a legend in the field. He was a young professor at the University of Chicago when I was there as a graduate student in the 1950s. His lack of interest in carbon-based superconductors discouraged many people from doing magnetic field studies on carbon-based superconductors. But many researchers did research on magnetism and superconductivity, especially after high-T_c superconductivity was discovered in 1986.

Junji Haruyama was one man not deterred by Matthias, and he decided to study both magnetism and superconductivity in carbon-based materials in his early career. He has pursued these studies since his early career and has become a major author in the field. In the last decade, research on nanocarbon materials has blossomed and currently, they materials are the focus of much interest. Therefore, a book on the current status of superconducting nanocarbons would be

of interest to this large community of potential readers. In this book, Junji Haruyama presents a review of the current understanding of this field based on his own research and that of others prominent in the field, emphasizing the special properties found in superconducting nanocarbons. The book also covers a broad range of other materials, presently an area of interesting developments.

Mildred Dresselhaus
Massachusetts Institute of Technology
Autumn 2014

Preface

Superconductors (SCs) are attractive materials in all respects for any community, especially academia and industry. They provide a deep insight into the physical properties of the condensed matter and also have useful applications as ultra-low-power-dissipation systems that can help resolve the present energy problems. Various types of SCs have been found to date. With respect to high transition temperature (T_c) over 40 K, CuO_2-based SCs and recently found Fe-based SCs have attracted considerable attention.

In particular, the progress of new carbon-based SCs (CBSCs) has been significant over the past decade. CBSCs had been investigated for a long time, especially in graphite-intercalated compounds (GICs). However, the T_c of CBSCs had been below only 1 K (such as in GICs), except in alkali metal–doped fullerene clusters, until 2004, when a Russian group discovered that doping diamond heavily with boron could result in realizing $T_c = 4$ K. This was amazing because until then diamond had been basically considered a wide-bandgap semiconductor or insulator. The following year, a Cambridge group found that calcium-intercalated graphite (CaC_6) could be a SC with $T_c = 11.5$ K. This was again incredible, because T_c of GICs had been below 1 K, as already mentioned. In 2006 and 2008, the editor's group from Japan discovered that arrays of entirely end-bonded multi-walled carbon nanotubes (CNTs) and thin films consisting of boron-doped single-walled CNTs could be SCs with $T_c = 12$ K. Because these findings revealed the correlation of superconductivity with one-dimensional (1D) electronic states and phenomena, they were highly interesting. Pressure-induced superconductivity at $T_c = 38$ K was also realized in Cs_3C_{60} in 2008. In 2013, a team of researchers from Hong Kong, Massachusetts Institute of Technology, and Japan demonstrated superconductivity in double-walled CNTs.

More findings about new CBSCs have appeared in the past decade and the field has developed rapidly. A small mass of carbon atom produces high phonon frequency and high Debye temperature, which are basically helpful in obtaining high T_c, according to the

Bardeen–Cooper–Schrieffer (BCS) theory. Moreover, different types of CB materials exhibit different physical origins for superconductivity, such as heavy carrier doping, 1D electronic states, coupling of intercalated foreign-atom layer with graphene layer, and Mott transition.

In particular, 1D physical properties of CNTs (such as Tomonaga–Luttinger liquid) obstruct the development of high-T_c superconductivity in some cases; however, a high T_c can be theoretically obtained if the 1D properties such as infinite 1D electronic density of states and coupling of a specified phonon mode (radial breathing phonon) with σ–π electrons are effectively used. A T_c even higher than 60 K has been predicted in CNTs by a Harvard group. Moreover, a theoretical study on Be- and Mg-intercalated graphite by a Japanese group also predicts $T_c > 60$ K. Therefore, it is highly expected that new CBSCs would open doors to high-T_c superconductivity as the third material group, following CuO_2- and Fe-based SCs, although the current highest T_c is still lower than 20 K except for the T_c of Cs_3C_{60}.

With 11 chapters authored by world-leading scientists, this book describes the basic physics and recent advances in experiments and theory of new CBSCs, such as diamond, GICs, graphene, CNTs, and silicon carbide, and discusses the above-mentioned issues with focus on superconductivity in CNTs.

I would like to thank all the contributors, without whose efforts this book would not have been possible. Unfortunately, Prof. Nikolai B. Kopnin, who is an author of the graphene superconductivity chapter, passed away on October 20, 2013, during a lecturing trip to Rome. I pray for the repose of his soul.

I hope this book will be a useful tool for students as well as experts who are trying to meet the challenge of achieving high-T_c superconductivity.

Junji Haruyama
Aoyama Gakuin University, Japan
Autumn 2014

Chapter 8

Theory for Reliable First-Principles Prediction of the Superconducting Transition Temperature

Yasutami Takada
Institute for Solid State Physics, University of Tokyo, Kashiwa, Chiba 277-8581, Japan
takada@issp.u-tokyo.ac.jp

A review is given for the theoretical framework to give a reliable prediction of the superconducting transition temperature (T_c) from first principles, together with a practical strategy for its application to actual materials with illustrations of the results of T_c calculated for superconductors in the weak-coupling region like the alkali- and alkaline-earth-intercalated graphites as well as those in the strong-coupling region like the alkali-doped fullerides.

8.1 Introduction

In quantum mechanics, a ground state is determined through a compromise between the kinetic energy (which makes particles itinerant) and the potential energy (which makes them localized). If the latter includes the interaction between particles, there appears

Carbon-Based Superconductors: Toward High-Tc Superconductivity
Edited by Junji Haruyama

ISBN 978-981-4303-30-9 (Hardcover), 978-981-4303-31-6 (eBook)
www.panstanford.com

a further complication due to their correlated motion. In elucidating the microscopic mechanism of superconductivity, this intrinsic complexity in quantum mechanics cannot be avoided but is even more intensified, specifically because superconductivity is a phenomenon in which an assembly of electrons, negatively charged particles with one-half spin, goes into the pair-condensed phase as a consequence of the dominance of some effective attractions between electrons mediated by either phonons, plasmons, spin-fluctuations, or orbital-fluctuations over the short-range Coulomb repulsions, indicating the necessity of deeply understanding and carefully investigating the physics of this charge–spin–phonon (-orbital) complex before making a reliable evaluation of the transition temperature T_c of this second-order phase transition. Thus one would imagine that the task of reliably calculating T_c must be formidably difficult, but the ultimate goal in the theoretical study of high-T_c superconductivity should be to construct a good theoretical framework for an accurate prediction of T_c; without such a theoretical tool, we could never conduct a research directly and intimately touched with the most salient feature of high-T_c materials, namely, the very feature that T_c becomes very high in those materials.

McMillan was the first to provide a rather successful scheme for predicting T_c in the phonon mechanism of superconductivity, starting from the microscopic electron–phonon coupled Hamiltonian. The scheme is known as the McMillan's formula [1], which was revised later by Allen and Dynes [2–4]. The formulae, both original and revised, are derived from the Eliashberg theory of superconductivity [5] and the task of a microscopic calculation of T_c in this framework is reduced to the evaluation of the so-called Eliashberg function $\alpha^2F(\omega)$ from the first-principles Hamiltonian, where $F(\omega)$ is the phonon density of states which may be observed by neutron diffraction. This function $\alpha^2F(\omega)$ enables us to obtain both the nondimensional electron–phonon coupling constant λ and the average phonon energy ω_0, through which we can give a first-principles prediction of T_c with an additional introduction of a phenomenological parameter μ^* (the Coulomb pseudopotential [6]) for the purpose of roughly estimating the effect of the short-range Coulomb repulsion between electrons on T_c.

At present, this framework is usually regarded as the standard one for making a first-principles prediction of T_c and widely used.

In fact, the superconducting mechanism of many (so-called weakly correlated) superconductors is believed to be clarified by employing this scheme. The key phonon modes to bring about superconductivity are identified by investigating the structure of $\alpha^2F(\omega)$. We can mention that superconductivity in MgB_2 with $T_c = 39$ K provides a very good example [7–10] to illustrate the power of this scheme. The case of CaC_6 with $T_c = 11.5$ K seems to constitute another recent example [11,12].

In spite of these and many other successful examples, however, this is not considered to be our ultimate scheme for calculating T_c from first principles, primarily because a phenomenological parameter μ^* is included in the theory. Actually, it cannot be regarded as the method of predicting T_c in the true sense of the word, if the parameter μ^* is determined so as to reproduce the observed T_c. Besides, as long as μ^* is employed to avoid a serious investigation of the effects of the Coulomb repulsion on superconductivity, this scheme cannot be applied to strongly correlated superconductors such as the high-T_c cuprates. Even in weakly or moderately correlated superconductors, this scheme cannot treat superconductivity originating from the Coulomb repulsion via charge, spin, and/or orbital fluctuations (namely, the electronic mechanism including the plasmon mechanism [13,14]). Furthermore, in this scheme, we cannot investigate the competition or the coexistence (or even the mutual enhancement due to the quantum-mechanical constructive interference effect) between the phonon and the electronic mechanisms.

The validity of the concept of μ^* is closely related to that of the Eliashberg theory itself; the theory is valid only if the Fermi energy of the superconducting electronic system, E_F, is much larger than ω_0. Note that under the condition of $E_F \gg \omega_0$, the dynamical response time for the phonon-mediated attraction ω_0^{-1} is much slower than that for the Coulomb repulsion E_F^{-1}, precluding any possible interference effects between two interactions, so that physically it is very plausible to separate them. After this separation, the Coulomb part (which was not anticipated to play a positive role in the Cooper-pair formation) has been simply treated in terms of a single parameter μ^*. Thus, for the purpose of searching for some positive role of the Coulomb repulsion in superconductivity, the concept of μ^* is irrelevant from the outset of the whole theory.

As for the condition of $E_F \gg \omega_0$, it must also be noted that such a condition is violated in some recently discovered superconductors in the phonon mechanism including the alkali-doped fullerenes with $T_c = 18$–38 K [15–18]. Once it is violated, we need to include higher-order corrections in the electron–phonon coupling (or the so-called vertex corrections Γ) in calculating the phonon-mediated attractive interaction [19]. Then, it is by no means clear whether we can fully treat the overall effect of various phonons in terms of the sum of the contribution from each phonon. This implies that the Eliashberg function $\alpha^2F(\omega)$ will not be appropriate enough to describe the phonon-mediated attraction because of possible interference effects among virtually-excited different phonon modes. As a consequence, λ will not be simply the sum of λ_i the contribution from the ith phonon, unless λ_i is small enough to validate the whole calculation in lowest-order perturbation.

If the condition of $E_F \gg \omega_0$ is violated, especially if E_F is about the same as ω_0, another complication occurs in treating the screening effect of the conduction electrons. In the usual calculation scheme from first principles, the static screening is assumed in calculating $\alpha^2F(\omega)$, but it does not reflect the actual screening process working during the formation of Cooper pairs. This subtle problem of screening is, of course, also closely related to the problem of the first-principles determination of μ^* and we will not be able to solve these problems unambiguously without confronting with a difficult task of treating both the Coulomb repulsion and the phonon-mediated attraction on the same footing in the calculation of the microscopic *dynamical* electron–electron effective interaction V.

In order to overcome the above-mentioned problems inherently associated with the Eliashberg theory, the first and natural option would be to improve on it by considering both the gap equation and the electron–electron effective interaction V in entire energy- and momentum-space with properly including the vertex corrections Γ in V and without separating the Coulomb repulsion from V. However, this will not be easily accomplished at least in the near future, partly because the demand for computational resources becomes too much in the solution of the full *non-local* and *dynamical* gap equation and partly because no controlled approximation scheme has been known for Γ for the superconducting state. (Note that the controlled scheme is known for the normal state [20,21].)

Fortunately, an alternative option has already been proposed by the extension of the density functional theory (DFT) to treat a superconducting state [22,23]. This theory provides a formally *exact* framework for calculating T_c from first principles by the solution of the gap equation only in momentum-space, setting aside the calculation of other physical quantities except for the one-electron density $n(\mathbf{r})$. Note that the effect of the Coulomb repulsion is properly included in this formulation without resort to the concept of μ^*. Therefore, we shall begin with making a very brief review of this DFT for superconductors (SCDFT) in Section 8.2. We shall point out that the central quantity in this framework is the pairing interaction K. Then in Section 8.3, we shall infer a concrete formula for K defined in terms of the Kohn–Sham (KS) orbitals in an inhomogeneous electron gas by reconsidering the gap equation for the homogeneous electron gas in the weak-coupling region with use of the Green's function method. The formula has not been proposed so far in the literature in SCDFT, but by its application to superconductivity in the alkali- and alkaline-earth-intercalated graphites [24,25], it turns out that this is indeed a very good approximate functional form for K. A prediction for the optimum value of T_c by using this functional form will be given for this class of materials. In Section 8.4, we shall consider a formula for K in the opposite limit, namely, in the strong-coupling region, especially for such superconductors with short coherence lengths as the alkali-doped fullerides [26]. By interpolating the formulae for K in these two limits, we shall propose a new functional form for K which is supposed to work well in the whole range of the coupling strength. The results of T_c obtained by its application to the fullerene superconductors and related materials will be shown in the last subsection of this section. Finally in Section 8.5, we shall conclude this short article, together with discussing the direction of future research.

8.2 SCDFT: Density Functional Theory for Superconductors

8.2.1 Hohenberg–Kohn–Sham Theorem

According to the basic theorem in the DFT due to Hohenberg and Kohn [27], all the physical quantities of an interacting electron system are uniquely determined, once its electronic density in

the ground state $n(\mathbf{r})$ is specified. This implies that every quantity including the exchange-correlation energy F_{xc} may be considered as a unique functional of $n(\mathbf{r})$. The ground-state density $n(\mathbf{r})$ itself can be determined by the calculation of the ground-state electronic density of the corresponding non-interacting reference system that is stipulated in terms of the KS equation [28]. The concept of the non-interacting reference system is of central importance in the KS algorithm and the core quantity in the KS equation is the exchange-correlation potential $V_{xc}(\mathbf{r})$, which is formally defined as the first-order functional derivative of $F_{xc}[n(\mathbf{r})]$ with respect to $n(\mathbf{r})$, namely, $V_{xc}(\mathbf{r}) = \delta F_{xc}[n]/\delta n(\mathbf{r})$. It must be noted that $V_{xc}(\mathbf{r})$ as well as each one-electronic wavefunction at ith level (usually called as "ith KS orbital") with its energy eigenvalue ε_i in the KS equation has no direct physical relevance; they are merely introduced for the mathematical convenience so as to obtain the *exact* $n(\mathbf{r})$ in the real many-electron system by exploitation of its one-to-one correspondence to the non-interacting reference system.

This basic Hohenberg–Kohn theorem can be applied not only to the normal ground state but also to the ordered one on the understanding that the order parameter itself in the ordered state is regarded as a functional of $n(\mathbf{r})$. In providing some approximate functional form for $F_{xc}[n]$ in actual calculations, however, it would be more convenient to treat the order parameter as an additional independent variable. For example, in considering the system with a collinear magnetic order, we usually employ the spin-dependent scheme in which the fundamental variable is not $n(\mathbf{r})$ but the spin-decomposed density $n_\sigma(\mathbf{r})$, leading to the spin-polarized exchange-correlation energy functional $F_{xc}[n_\sigma]$, based on which the spin-dependent exchange-correlation potential is defined to specify the spin-dependent KS equation for determining $n_\sigma(\mathbf{r})$ from first principles.

8.2.2 Gap Equation in SCDFT

In an essentially similar way, in treating superconductivity in the framework of DFT, it would be better to construct the energy functional with employing both $n(\mathbf{r})$ and the electron-pair density (or the superconducting order parameter) $\chi(\mathbf{r},\mathbf{r}')(\equiv\langle\Psi_\uparrow(\mathbf{r})\Psi_\downarrow(\mathbf{r}')\rangle)$ as basic variables [22,23], leading to the pair density–dependent

exchange-correlation energy functional $F_{xc}[n(\mathbf{r}), \chi(\mathbf{r}, \mathbf{r}')]$, where $\Psi_\sigma(\mathbf{r})$ is the annihilation operator of σ-spin electron field at position $\mathbf{r}$. In accordance with this addition of the order parameter as a fundamental variable to DFT, not only the exchange-correlation potential $V_{xc}(\mathbf{r})$ but also the exchange-correlation pair-potential $\Delta_{xc}(\mathbf{r}, \mathbf{r}') = -\delta F_{xc}[n, \chi]/\delta\chi^*(\mathbf{r}, \mathbf{r}')$ appear in an extended KS equation. A beautiful point in this DFT for superconductors (SCDFT) is that the extended KS equation can be written in the form of the Bogoliubov–de Gennes equation appearing in the conventional theory for inhomogeneous superconductors [29]. Just as is the case with $V_{xc}(\mathbf{r})$, $\Delta_{xc}(\mathbf{r}, \mathbf{r}')$ has no direct physical meaning, but in principle, if the exact form of $F_{xc}[n, \chi]$ is known, the solution of the extended KS equation gives us the exact result for $\chi(\mathbf{r}, \mathbf{r}')$, containing all the effects of the Coulomb repulsion including the one usually treated phenomenologically through the concept of μ^*. As a result, we can determine the exact T_c by the calculation of the highest temperature below which a non-zero solution for $\chi(\mathbf{r}, \mathbf{r}')$ can be found.

In this framework of SCDFT, we can formally write down the fundamental gap equation to determine T_c exactly as

$$\Delta_j = -\sum_{j'} \frac{\Delta_{j'}}{2\varepsilon_{j'}} \tanh\frac{\varepsilon_{j'}}{2T_c} K_{jj'}, \tag{8.1}$$

where Δ_j is the gap function associated with jth KS orbital. In just the same way as its energy eigenvalue ε_j (which is measured relative to the chemical potential), Δ_j is not the quantity to be observed experimentally but just introduced for the mathematical convenience so as to obtain the exact T_c by solving this BCS-type equation, Eq. (8.1). Similarly, the pairing interaction $K_{jj'}$, defined as the second-order functional derivative of $F_{xc}[n, \chi]$ with respect to χ^* and χ, has not any direct physical meaning, either, although this is a quantity of primary importance in this gap equation or even in the whole framework of SCDFT.

Three comments are in the following order: (i) The functional derivatives of $F_{xc}[n, \chi]$ might not be well-defined, as anticipated by remembering the notorious energy-gap problem in semiconductors and insulators [30–32], but as is ordinarily the case, we shall assume

---

Throughout this article, we use units in which $\hbar = k_B = 1$.

that $K_{jj'}$ is a well-defined quantity. (ii) In this formal derivation in SCDFT, the dynamical (or ω-dependent) nature in the electron–electron multiple scatterings does not manifest itself in either the gap equation or the pairing interaction, in sharp contrast with the Eliashberg theory. For this reason, many people cast doubt on whether the physics leading to μ^* is actually taken into account in SCDFT. However, due to the fact that there is a very good correspondence between this gap equation and the one in the G_0W_0 approximation to the Elishaberg theory, as will be shown in the next section, we find that it is possible to include the full dynamical processes in the Cooper-pair formation in the framework of SCDFT, as long as the form of $K_{jj'}$ is properly chosen. (iii) At $T = T_c$, $K_{jj'}$ is evaluated at $\chi = 0$. Thus $K_{jj'}$ must be a functional of only the normal-state electronic density $n(\mathbf{r})$. Note that each KS orbital, j or j', determined in the normal state may be regarded as a functional of $n(\mathbf{r})$, justifying the view that $K_{jj'}$ at $T = T_c$ is eventually a functional of $n(\mathbf{r})$ in the normal state.

8.2.3 Application and Discussion

This formal framework of SCDFT was not applied to actual superconductors before the year 2005 when an attempt was made to provide a concrete approximate form for $F_{xc}[n, \chi]$ in which the contribution from the phonon-mediated attraction was explicitly included up to the level of the Eliashberg theory [33]. Since then many (but mostly weakly correlated) superconductors have been analyzed rather successfully in this framework [34–39].

In the judgement of the present author, the presently available form for $F_{xc}[n, \chi]$ or the one for $K_{jj'}$ contains the information equivalent to that included in the Eliashberg theory for the part of the phonon-mediated attraction, indicating that no vertex corrections are considered in this treatment (amounting to the very insufficient treatment of the strong polaronic effect), while for the part of the Coulomb repulsion, it contains only very crude physics; the screening effect is treated in the Thomas–Fermi static-screening approximation, or the result in the random phase approximation (RPA) only in the static and the long-wavelength limit, neglecting both the dynamical and non-local feature in the effects of the Coulomb repulsion. This clearly indicates that the Coulomb repulsion is not treated on the same footing as the phonon-mediated

attraction and this approximation for the Coulomb part will be just good for describing the physics represented by μ^* at usual metallic densities (or $r_s \approx 2$ with r_s the conventional non-dimensional density parameter) from first principles, but it fails to take care of the detailed dynamical nature of the screening effect, especially, the positive role of the plasmons in superconductivity for lower densities (or larger r_s) [13,14]. Furthermore, the presently available form for $F_{xc}[n, \chi]$ or $K_{jj'}$ does not allow to discuss other types of the electronic mechanisms such as the spin-fluctuation one, either. In view of these fundamental problems, it is absolutely necessary to derive a much better approximate functional form for $K_{jj'}$ for the purpose of investigating the electronic mechanisms in the absence/presence of the phonon mechanism.

It would be appropriate here to make rather a general comment on numerical errors. Currently, calculations of the normal-state properties are done in either the local-density approximation (LDA) or the generalized-gradient approximation (GGA) [40] to $F_{xc}[n(\mathbf{r})]$ in DFT. We usually anticipate that errors in the calculated results are of the order of 1 eV and 0.3 eV for LDA and GGA, respectively, and those errors are much larger than that expected in quantum chemistry ($\approx$0.05 eV). Now in the usual procedure in SCDFT, the calculation of T_c (which is of the order of 0.001 eV in general) is done simultaneously with that of the normal state and thus the error for T_c might be of the same order as that for the normal state properties, implying that it might become much larger than T_c itself.

This unfavorable situation may be avoided, if we take the following two-stage strategy for the calculation of T_c for a family of superconducting materials in consideration; in the first stage, combined with available experimental results on the normal state, we establish a good model system representing this family of superconductors by making a first-principles band-structure calculation and then in the second stage, we evaluate T_c based on the model system not only for reproducing the experimental T_c but also for suggesting not yet synthesized but promising superconductors with higher T_c in this family. In the rest of this article, we shall discuss two families of the carbon-based superconductors for which T_cs are calculated and predicted in accordance with this two-stage strategy.

8.3 G_0W_0 Approximation with Application to Graphite Intercalation Compounds

8.3.1 Pairing Interaction in the Weak-Coupling Region

The three-dimensional (3D) homogeneous electron gas has been known to be a very useful system in constructing a successful functional form for $V_{xc}(\mathbf{r})$ in either LDA or GGA by its study with use of various powerful many-body techniques including quantum Monte Carlo simulations. In view of this success, we shall study superconductivity in the same system with the conventional Green's function method in order to infer a good functional form for the pairing interaction $K_{jj'}$ in Eq. (8.1) that will be exact in the weak-coupling limit.

In a homogeneous system, momentum $\mathbf{p}$ is always a good quantum number and an electron can be specified by $\mathbf{p}$ and spin σ. If we write the electron annihilation operator by $c_{\mathbf{p}\sigma}$ the Hamiltonian H of the 3D electron-gas system coupled with phonons is given by

$$\begin{aligned} H &= H_e + H_{ph} \\ &= \sum_{\mathbf{p}\sigma} \varepsilon_{\mathbf{p}} c^+_{\mathbf{p}\sigma} c_{\mathbf{p}\sigma} + \frac{1}{2} \sum_{\mathbf{q}\neq 0} \sum_{\mathbf{p}\sigma} \sum_{\mathbf{p}'\sigma'} V_0(\mathbf{q}) c^+_{\mathbf{p}\sigma} c^+_{\mathbf{p}'\sigma'} c_{\mathbf{p}'-\mathbf{q}\sigma} c_{\mathbf{p}+\mathbf{q}\sigma'} + H_{ph}, \end{aligned} \tag{8.2}$$

where $\varepsilon_{\mathbf{p}} (\equiv \mathbf{p}^2/2m^* - \mu)$ is the bare one-electron dispersion relation with m^* the band mass and μ the chemical potential, $V_0(\mathbf{q}) (\equiv 4\pi e^2/\varepsilon_\infty \mathbf{q}^2)$ is the bare Coulomb repulsion with ε_∞ the optical dielectric constant, and H_{ph} represents all contributions containing the phonon operators. For the time being, there is no need of our specifying a concrete form for H_{ph}.

In the thermal Green's function method, we can treat superconductivity by introducing the abnormal thermal Green's function $F(\mathbf{p}, i\omega_p)$, which is defined at temperature T by

$$F(\mathbf{p}, i\omega_p) = -\int_0^{1/T} d\tau e^{i\omega_p \tau} \left\langle T_\tau c_{\mathbf{p}\uparrow}(\tau) c_{-\mathbf{p}\downarrow} \right\rangle. \tag{8.3}$$

Here ω_p is the fermion Matsubara frequency, defined by $\pi T(2p+1)$ with an integer p. At $T = T_c$ where the second-order superconducting

phase transition occurs, this function satisfies the following formally exact gap equation:

$$F(\mathbf{p},i\omega_p)=-G(\mathbf{p},i\omega_p)G(-\mathbf{p},-i\omega_p)T_c\sum_{\omega_{p'}}\sum_{\mathbf{p}'}\tilde{J}(\mathbf{p},\mathbf{p}';i\omega_p,i\omega_{p'})F(\mathbf{p}',i\omega_{p'}), \tag{8.4}$$

where $G(\mathbf{p}, i\omega_p)$ is the normal thermal Green's function and $\tilde{J}(\mathbf{p},\mathbf{p}';i\omega_p,i\omega_{p'})$ is the irreducible electron–electron effective interaction.

Let us assume that the effect of interaction is weak, so that it would be enough to retain the terms only in lowest order in the interaction. If we adopt the same assumption in the calculation of the normal-state properties in the Green's function approach, we are led to the so-called G_0W_0 approximation or the one-shot *GW* approximation in terminology prevailing in the present-day first-principles calculation community, where W is the effective interaction between electrons including both the Coulomb and the phonon-mediated interactions and W_0 represents W in RPA. Incidentally, in the same kind of terminology, the Eliashberg theory corresponds to the *GW* approximation. Historically, Cohen was the first to evaluate T_c in degenerate semiconductors on the level of the G_0W_0 approximation [41,42]. Unfortunately the pairing interaction is not correctly derived in his theory, as explicitly pointed out by the present author [43] who, instead, by consulting the pertinent work of Kirzhnits et al. [44], has succeeded in obtaining the correct pairing interaction [13], the result of which will be reiterated in the following.

In the G_0W_0 approximation, we replace $G(\mathbf{p}, i\omega_p)$ by the bare one $G_0(\mathbf{p}, i\omega_p)[\equiv (i\omega_p - \varepsilon_{\mathbf{p}})^{-1}]$ in Eq. (8.4) and consider the case in which $\tilde{J}(\mathbf{p},\mathbf{p}';i\omega_p,i\omega_{p'})$ is well-approximated as a function of only the variables $(\mathbf{p}-\mathbf{p}', i\omega_p - i\omega_{p'})$ to write

$$\tilde{J}(\mathbf{p},\mathbf{p}';i\omega_p,i\omega_{p'})=V(\mathbf{p}-\mathbf{p}',i\omega_p-i\omega_{p'}), \tag{8.5}$$

as is usually the case for W_0 the effective interaction in RPA, though we do not intend to confine ourselves to RPA at this stage. By substituting Eq. (8.5) into Eq. (8.4), we obtain the gap equation in the G_0W_0 approximation as

$$F(\mathbf{p},i\omega_p) = -G_0(\mathbf{p},i\omega_p)G_0(-\mathbf{p},-i\omega_p)T_c\sum_{\omega_{p'}}\sum_{\mathbf{p}'}V(\mathbf{p}-\mathbf{p}';i\omega_p-i\omega_{p'})F(\mathbf{p}',i\omega_{p'}). \tag{8.6}$$

Then, by making an analytic continuation on the ω plane to transform $F(p, i\omega_p)$ to the retarded function $F^R(\mathbf{p}, \omega)$ on the real-ω axis and using the general relation due to the causality principle as

$$V^R(\mathbf{q},\omega) = V_0(\mathbf{q}) - \int_0^\infty \frac{d\Omega}{\pi} \frac{2\Omega}{\omega^2 - \Omega^2 + i\eta} \mathrm{Im}V^R(\mathbf{q},\Omega), \tag{8.7}$$

with η a positive infinitesimal, we end up with a gap equation for $F^R(\mathbf{p}, \omega)$. Finally, by taking the imaginary parts in both sides of the gap equation and integrating over the ω variable, we are led to an equation depending only on the momentum variable $\mathbf{p}$. More specifically, the equation can be cast into the following BCS-type gap equation:

$$\Delta_{\mathbf{p}} = -\sum_{\mathbf{p}'} \frac{\Delta_{\mathbf{p}'}}{2\varepsilon_{\mathbf{p}'}} \tanh\frac{\varepsilon_{\mathbf{p}'}}{2T_c} K_{\mathbf{p},\mathbf{p}'}, \tag{8.8}$$

where the gap function $\Delta_{\mathbf{p}}$ and the pairing interaction $K_{\mathbf{p},\mathbf{p}'}$ are, respectively, defined as

$$\Delta_{\mathbf{p}} \equiv 2|\varepsilon_{\mathbf{p}}| \int_0^\infty \frac{d\omega}{\pi} \mathrm{Im}F^R(\mathbf{p},\omega), \tag{8.9}$$

and

$$\begin{aligned} K_{\mathbf{p},\mathbf{p}'} &\equiv V_0(\mathbf{p}-\mathbf{p}') + \int_0^\infty \frac{2}{\pi} d\Omega \frac{\mathrm{Im}V^R(\mathbf{p}-\mathbf{p}',\Omega)}{\Omega + |\varepsilon_{\mathbf{p}}| + |\varepsilon_{\mathbf{p}'}|} \\ &= \int_0^\infty \frac{2}{\pi} d\Omega \frac{|\varepsilon_{\mathbf{p}}| + |\varepsilon_{\mathbf{p}'}|}{\Omega^2 + (|\varepsilon_{\mathbf{p}}| + |\varepsilon_{\mathbf{p}'}|)^2} V(\mathbf{p}-\mathbf{p}', i\Omega). \end{aligned} \tag{8.10}$$

With use of $K_{\mathbf{p},\mathbf{p}'}$ thus derived, we can determine T_c as an eigenvalue of Eq. (8.8), indicating that we have obtained a scheme in which T_c is given directly from the microscopic one-electron dispersion relation $\varepsilon_{\mathbf{p}}$ and the effective electron–electron interaction $V(\mathbf{q}, i\Omega)$. Because there is no need to separate the phonon-mediated attraction from the Coulomb repulsion in $V(\mathbf{q}, i\Omega)$ and the dynamical nature of the interaction is fully taken into account, we can properly treat the physics leading to μ^* from first principles with use of this scheme.

The very definition of the gap function $\Delta_{\mathbf{p}}$ in Eq. (8.9) indicates that $\Delta_{\mathbf{p}}$ does not correspond to the physical energy gap except in the weak-coupling limit. Similarly, $K_{\mathbf{p},\mathbf{p}'}$ is not a physical entity, although V is the physical effective interaction. Both quantities are introduced for the

mathematical convenience so as to make T_c invariant in transforming Eq. (8.4) into Eq. (8.8). The key point here is that we need not solve the full gap Eq. (8.4) but much simpler one (8.8) in order to obtain T_c in Eq. (8.4). Of course, if we want to know the physical gap function rather than $\Delta_{\mathbf{p}}$ to compare with experiment, we need to solve the full gap equation, Eq. (8.4), with T_c determined by Eq. (8.8).

Although the spin-singlet pairing has been assumed in the derivation of Eq. (8.8), no assumption is made on the dependence of the gap function on angular valuables, so that this gap equation can treat any kind of the pairing anisotropy in the gap function, indicating that it can be applied to s-wave, d-wave, ..., and even their mixture like (s+d)-wave superconductors.

Now, let us compare Eq. (8.8) with Eq. (8.1). Since the KS orbitals, j and j', can be specified by momenta, $\mathbf{p}$ and $\mathbf{p}'$, respectively, in a homogeneous system and $\varepsilon_{j'} = \varepsilon_{\mathbf{p}'}$, we may regard that these two equations are essentially the same, suggesting that we may give a concrete functional form for $K_{jj'}$ with use of energies of the KS orbitals, ε_j and $\varepsilon_{j'}$, as

$$K_{jj'} = \int_0^\infty \frac{2}{\pi} d\Omega \frac{|\varepsilon_j| + |\varepsilon_{j'}|}{\Omega^2 + (|\varepsilon_j| + |\varepsilon_{j'}|)^2} V_{jj'}(i\Omega). \tag{8.11}$$

Here $V_{jj'}(i\Omega)$ is the dynamical effective interaction working for the scattering process from a pair of electrons in (j, j^*) orbitals to another pair in (j', j'^*) orbitals, as schematically shown in Fig. 8.1 (By j^* we mean the time-reversed KS orbital of j.) We should calculate this $V_{jj'}(i\Omega)$ on the understanding that it must be derived from the first-principles Hamiltonian expanded with use of a complete set of the KS orbitals as an orthnormal basis. Together with the gap equation, Eq. (8.1), and the KS orbitals obtained in the normal state by the conventional DFT-based method, Eq. (8.11) constitutes a basic framework for a first-principles calculation of T_c for inhomogeneous weak-coupling superconductors.

8.3.2 Superconductivity in Polar Semiconductors

In order to assess the quality of this basic framework in the G_0W_0 approximation for calculating T_c from the first principle, we have applied it to polar degenerate semiconductors, specifically, the doped $SrTiO_3$ and compared the calculated results with experiments [43].

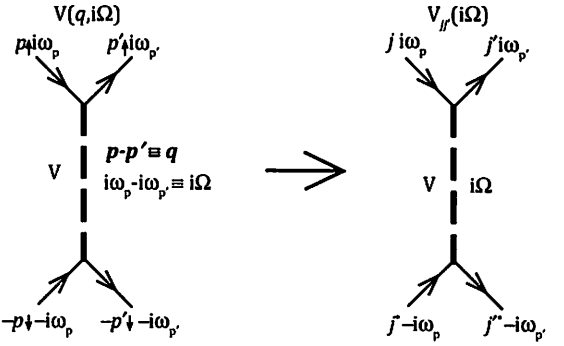

Figure 8.1 Schematic representation of the dynamical effective interaction $V_{jj'}(i\Omega)$ as inferred from $V(\mathrm{q}, i\Omega)$.

This material is an insulator and exhibits ferroelectricity under a uniaxial stress of about 0.16 GPa along the [100] direction, but it turns into an *n*-type semiconductor by either Nb doping or oxygen deficiency, whereby the conduction electrons are introduced in the 3D band of Ti around the Γ point with the band mass of $m^* \approx 1.8\, m_e$ (m_e: the mass of a free electron). At low temperatures, superconductivity appears and the observed T_c shows interesting features; T_c depends strongly on the electron concentration n and it is optimized with $T_c \approx 0.3$ K at $n \approx 10^{20}$ cm^{-3}. Its dependence on the pressure is unsual; T_c decreases rather rapidly with hydrostatic pressures, but it increases with the [100] uniaxial stress, implying that the superconductivity is brought about by the polar-coupling phonons associated with the stress-induced ferroelectric phase transition.

Taking those situations into account, we have assumed that the material is well represented by a model of the 3D electron–gas system coupled with polar-optical phonons in which a concrete form for $V(\mathbf{q}, i\Omega)$ can be derived in RPA as

$$V(\mathbf{q},i\Omega)=\frac{4\pi e^2}{\varepsilon(\mathbf{q},i\Omega)\mathbf{q}^2}, \tag{8.12}$$

with the dielectric function in the electron–optical phonon system as

$$\varepsilon(\mathbf{q},i\Omega)=\varepsilon_\infty+\frac{4\pi e^2}{\mathbf{q}^2}\Pi_0(\mathbf{q},i\Omega)+[\varepsilon_0(\mathbf{q})-\varepsilon_\infty]\frac{\omega_t(\mathbf{q})^2}{\omega_t(\mathbf{q})^2+\Omega^2}, \tag{8.13}$$

where $\Pi_0(\mathbf{q}, i\Omega)$ is the polarization function in RPA (or the Lindhard function) for the 3D electron gas, $\omega_t(\mathbf{q})$ is the energy dispersion of the transverse optical phonon, and $\varepsilon_0(\mathbf{q})$ is the static non-local dielectric function, which is determined with use of the static dielectric constant ε_0 and $\omega_t(\mathbf{q})$ as

$$\varepsilon_0(\mathbf{q}) = \varepsilon_0 \frac{\omega_t(0)^2}{\omega_t(\mathbf{q})^2}. \tag{8.14}$$

The dispersionless longitudinal-phonon energy ω_1 is related to the transverse-phonon energy in the long-wavelength limit $\omega_t(0)$ through the Lyddane–Sachs–Teller relation as

$$\omega_1 = \sqrt{\frac{\varepsilon_0}{\varepsilon_\infty}}\,\omega_t(0). \tag{8.15}$$

By substituting $V(\mathbf{q}, i\Omega)$ in Eq. (8.12) into Eq. (8.10) and using the experimental data to determine the values of parameters like ε_0 and ε_∞ as well as the dispersion relation for $\omega_t(\mathbf{q})$, we have obtained T_c directly from a microscopic model and the results of T_c are in surprisingly good quantitative agreement with experiment, as shown in Fig. 8.2. The unusual dependence of T_c on the pressure is also reproduced well, though it is not shown here. (For interested readers, refer to the original paper [43].) This success indicates that the present framework including the adoption of RPA for calculating the effective interaction is useful and appropriate at least in the polar-coupled phonon mechanism in which the contribution from the long-range part of the interaction dominates over that from the short-range one.

8.3.3 Graphite Intercalation Compounds

8.3.3.1 Historical survey

The graphite intercalation compounds (GICs) have been investigated for a long time from physical, chemical, and technological points of view [47–50]. Among various kinds of GICs, special attention has been paid to the first-stage metal compounds, mainly because superconductivity is observed only in this class of GICs, the chemical formula of which is written as MC_x, where M represents either an

alkali atom (such as Li, K, Rb, and Cs) or an alkaline-earth atom (such as Ca, Sr, and Yb) and x is 2, 6, or 8. The crystal structure of MC_x is shown in Fig. 8.3(a), in which the metal atom M occupies the same spot in the framework of a honeycomb lattice at every $(x/2)$ layers of carbon atoms.

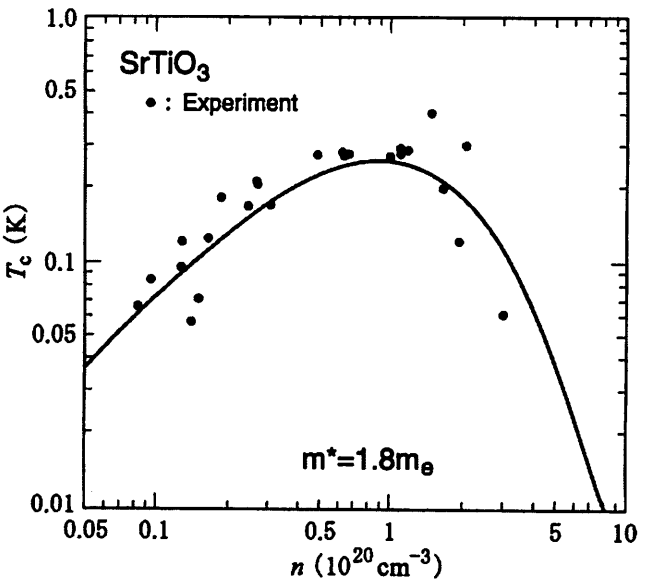

Figure 8.2 Calculated results for T_c in semiconducting $SrTiO_3$ as a function of the electron density n (the solid curve [43]), together with the experimental results (the filled circles [45]. See also [46].)

The first discovery of superconductivity in GICs was made in KC_8 with the T_c of 0.15 K in 1965 [51]. In pursuit of higher T_c, various GICs were synthesized, mostly working with the alkali metals and alkali-metal amalgams as intercalants, from the late 1970s to the early 1990s [52–59], but only a limited success was achieved at that time; the highest attained T_c was around 2–5 K in the last century. For example, it is 1.9 K in LiC_2 [60].

A breakthrough occurred in 2005 when T_c went up to 11.5 K in CaC_6 [61,62] (and even to 15.4 K under pressures up to 7.5 GPa [63]). In other alkaline-earth GICs, the values of T_c are 6.5 K and 1.65 K for YbC_6 [61] and SrC_6 [64], respectively. Since then, very

intensive experimental studies have been made in those and related compounds [62–66]. Theoretical studies have also been performed mainly by making state-of-the-art first-principles calculations of the electron–phonon coupling constant λ to account for the observed value of T_c for each individual superconductor [11,12,34,67]. Those experimental/theoretical works have elucidated that, although there are some anisotropic features in the superconducting gap, the conventional phonon-driven mechanism to bring about s-wave superconductivity applies to those compounds. This picture of superconductivity is confirmed by, for example, the observation of the Ca isotope effect with its exponent $\alpha = 0.50$, the typical BCS value [68].

In spite of all those efforts and the existence of such a generally accepted picture, we need to know more important and fundamental issues that include:

i. Standard model: Can we understand the mechanism of superconductivity in both alkali GICs with T_c in the range 0.01–1.0 K and alkaline-earth GICs with T_c in the range 1–10 K from a unified point of view? In other words, is there any standard model for superconductivity in GICs with T_c ranging over three orders of magnitude?
ii. Key parameters to control T_c: What is the actual reason why T_c is enhanced so abruptly (or by about a hundred times) by just substituting K by Ca the atomic mass of which is almost the same as that of K? In terms of the standard model, what are the key controlling physical parameters to bring about this huge enhancement of T_c? This change of T_c from KC_8 to CaC_6 is probably the most important issue in exploring superconductivity across the entire family of GICs.
iii. Optimum T_c: Is there any possibility to make a further enhancement of T_c in GICs? If possible, what is the optimum value of T_c expected in the standard model and what kind of atoms should be intercalated to realize the optimum T_c in actual GICs?

Recently these three issues have been satisfactorily addressed by the present author [24,25], as shall be explained one by one in the following three subsections.

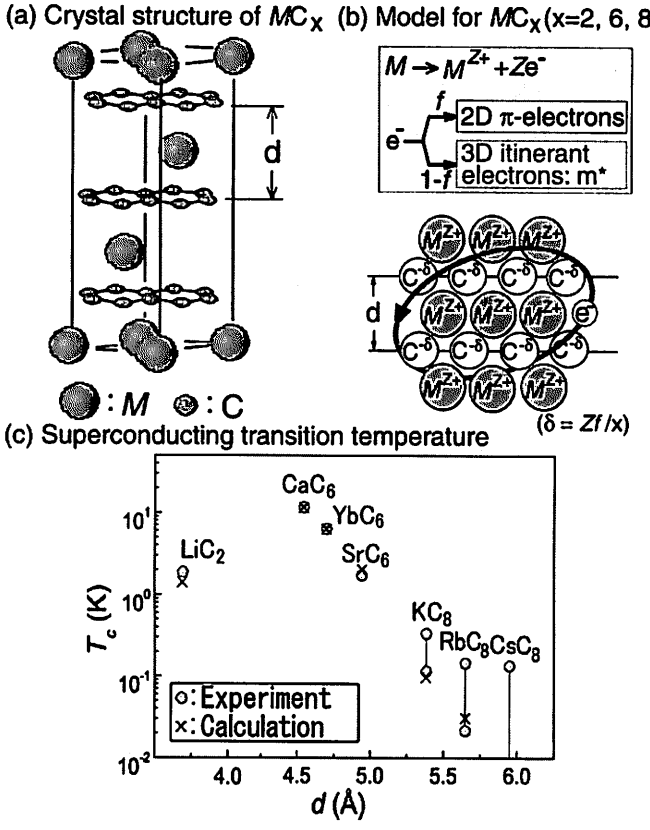

Figure 8.3 (a) Crystal structure of MC_x(ix = 2,6,8). The case of $x = 6$ is illustrated here, in which the metal atoms, *M*s, are arranged in a rhombohedral structure with the $\alpha\beta\gamma$stacking sequence, implying that *M* occupies the same spot in the framework of a graphene lattice at every three layers (or at the distance of 3d with *d* the distance between the adjacent graphite layers). (b) Simplified model to represent MC_x superconductors. We consider the attraction between the 3D electrons in the interlayer band induced by polar-coupled charge fluctuations of the cation M^{z+} and the anion $C^{-\delta}$. (c) T_c in the first-stage alkali- and alkaline-earth-intercalated graphites plotted as a function of *d*. The solid circles show the experimental results, while the crosses the calculated ones in the G_0W_0 approximation for the model represented in (b) with suitable values for the parameters such as Z, m^*, and f for each MC_x.

8.3.3.2 Standard model for intercalated graphite superconductors

The usual DFT-based self-consistent band-structure calculation is useful in elucidating the electronic structures of GICs in the normal state, basically because GICs are not strongly correlated materials. According to such a calculation, no essential qualitative difference is found between alkali- and alkaline-earth GICs. The main common features among these GICs may be summarized as follows:

First of all, each intercalant metal atom in MC_x acts as a donor and changes from a neutral atom M to an ion M^{Z+} with valence Z. Then, the valence electrons released from M will transfer either to the graphite π bands or the 3D band composed of the intercalant orbitals and the graphite interlayer states [69–71]. We shall define the factor f as the branching ratio between these two kinds of bands. Namely, Zf and $Z(1-f)$ electrons will go to the π and the 3D bands, respectively. The electrons in the graphite π bands are characterized by the two-dimensional (2D) motion with a linear dispersion relation (known as a Dirac cone in the case of graphene) on the graphite layer.

The dispersion relation of the graphite interlayer band is very similar to that of the 3D free-electron gas, folded into the Brillouin zone of the graphite [67]. Thus its energy level is very high above the Fermi level in the graphite, because the amplitude of the wavefunction for this band is small on the carbon atoms. In MC_x, on the other hand, the cation M^{Z+} is located in the interlayer position where the amplitude of the wavefunctions is large, lowering the energy level of the interlayer band below the Fermi level. The dispersion of the interlayer band is modified from that of the free-electron gas because of the hybridization with the orbitals associated with M, but generally it is well approximated by $\varepsilon_{\mathbf{p}} = \mathbf{p}^2/2m^* - E_F$ with an appropriate choice of the effective band mass m^* and the Fermi energy E_F. Here the value of m^* depends on M; in alkali GICs, the hybridization occurs with s-orbitals, allowing us to consider that $m^* = m_e$, while in alkaline-earth GICs, the hybridization with d-orbitals contributes much, leading to $m^* \approx 3\ m_e$ in both CaC_6 and YbC_6, as revealed by the band-structure calculation [11,12].

The value of f, which determines the branching ratio Zf: $Z(1-f)$, can be obtained by the self-consistent band-structure calculation. In KC_8, for example, it is known that f is around 0.6 [72,73]. On the

other hand, f is about 0.16 in CaC_6, making the electron density in the 3D band n increase very much [12]. This increase in n is easily understood by the fact that the energy level of the interlayer band is much lower with Ca^{2+} than with K^+. The concrete numbers for n are 3.5×10^{21} cm^{-3} and 2.4×10^{22} cm^{-3} for KC_8 and CaC_6, respectively, in which the difference in both d and x is also taking into account.

As inferred from experiments [48,67] and also from the comparison of T_c calculated for each band [74], it has been concluded that only the 3D interlayer band is responsible for superconductivity. Note that LiC_6 does not exhibit superconductivity because no carriers are present in the 3D interlayer band, although the properties of LiC_6 are generally very similar to those of other superconducting GICs in the normal state.

With the above-mentioned common features in mind, we can think of a simple model of a 3D electron gas coupled with phonons for the GIC superconductors, which is schematically shown in Fig. 8.3(b). In order to give some idea about the mechanism to induce an attraction between 3D electrons in this model, let us imagine how each conducting 3D electron sees the charge distribution of the system. First of all, there are positively charged metallic ions M^{Z+} with its density n_M, given by $n_M = 4/3\sqrt{3}a^2dx$, where a is the bond length between C atoms on the graphite layer (which is 1.419 Å). Note that with use of this n_M, the density of the 3D electrons n is given by $(1-f)Zn_M$. There are also negatively charged carbon ions $C^{-\delta}$ with δ given by $\delta = fZ/x$ on the average. Therefore, the 3D electrons will feel a large electric field of the polarization wave coming from oscillations of M^{Z+} and $C^{-\delta}$ ions created by either out-of-phase optical or in-phase acoustic phonons.

Although there are some additional complications originating from the combined contributions from both optical and acoustic modes in the layered-lattice system, this coupling of an electron with the polar phonons is essentially similar to the one we have already considered in the previous subsection. Thus, it is straightforward to derive the effective interaction $V(\mathbf{q}, i\Omega)$ in RPA in which the bare Coulomb repulsion and the polar-phonon-mediated attraction are treated on the same footing with the screening effects of both the 2D and 3D electrons. A concrete form for $V(\mathbf{q}, i\Omega)$ will not be given here, but for its detailed derivation we refer to the original paper [74] in which exactly the same model as presented in Fig. 8.3(b) was

proposed in as early as 1982 by the present author for analyzing superconductivity in alkali GICs.

8.3.3.3 Key physical parameters to control superconductivity

We have evaluated T_c from the first principle by using $V(\mathbf{q}, i\Omega)$ thus obtained to solve the gap equation (8.8). In Fig. 8.3(c), the calculated results of T_c for various MC_x are plotted by the crosses with the choice of suitable values for the parameters such as Z, m^*, and f for each material. As we see, the agreement between theory and experiment is quite excellent across the entire family of GICs, implying that our simple model may well be regarded as the standard one for describing the mechanism of superconductivity in GICs.

In order to identify the controlling physical parameters to enhance T_c in CaC_6 by hundred times from that in KC_8, let us compare the values for the physical parameters between the two materials: (i) The valence Z; because the valence changes from monovalence to divalence, the value of Z in CaC_6 is doubled to make the bare polar phonon-mediated attraction (which is in proportion to Z^2) stronger by four times. (ii) The interlayer distance d; it decreases from 5.42 Å to 4.524 Å, so that the 3D electron density n increases in CaC_6. (iii) The factor f to determine the branching ratio; it decreases from about 0.6 to 0.16, which also makes a further increase in n. (iv) The effective band mass for the 3D interlayer band m^*; it increases from m_e to about $3m_e$, leading to a large enhancement of the density of states at the Fermi level. (v) The atomic number of the ion A; it changes only from 39.1 in K to 40.1 in Ca. Thus the energies of phonons hardly change.

We have recalculated T_c by shifting each parameter, one by one, from the above-mentioned respective physical value and have found that two parameters, namely, Z and m^*, are very important in controlling the overall magnitude of T_c. In fact, T_c is enhanced by one order of magnitude from that in KC_8 by doubling Z from $Z = 1$ to $Z = 2$ with m^* kept to be m_e. A further enhancement of T_c by another one order is seen by tripling m^* from m_e to $3m_e$, with Z kept to be $Z = 2$. Thus, we may conclude that the enhancement of T_c in CaC_6 by about a hundred times from that in KC_8 is brought about by the combined effects of doubling Z and tripling m^*. In this respect, the actual value of m^* is very important. Appropriateness of $m^* \approx 3m_e$ is confirmed not only from the band-structure calculations [11,12], but also from

the measurement of the electronic specfic heat [65] compared with the corresponding one for KC_8 [75].

A note will be added here on the case of YbC_6; the basic parameters such as Z, f, and m^* for YbC_6 are about the same as those for CaC_6, according to the band-structure calculation. The only big difference can be seen in the atomic mass; Yb (in which $A = 173.0$) is much heavier than that of Ca by about four times, indicating weaker couplings between electrons and polar phonons as just in the case of comparison between KC_8 and RbC_8 or CsC_8. In fact, T_c for YbC_6 becomes about one half of the corresponding result for CaC_6, which agrees well with experiment. One way to understand this difference is to regard it as an isotope effect with $\alpha \approx 0.5$ [11].

8.3.3.4 Prediction of optimum T_c

As we have seen so far, our standard model could have predicted $T_c = 11.5$ K for CaC_6 in 1982 and it is judged that its predictive power is very high. Incidentally, the author did not perform the calculation of T_c for CaC_6 at that time, partly because he did not know a possibility to synthesize such GICs, but mostly because the calculation cost was extremely high in those days; a rough estimate shows that there is acceleration in computers by at least a millon times in the past three decades. This huge improvement on computational environments is surely a boost to making such a first-principles calculation of T_c in the G_0W_0 approximation.

We have explored the optimum T_c in the whole family of GICs by widely changing various parameters involved in the microscopic Hamiltonian of the standard model. Examples of the calculated results of T_c are shown in Fig. 8.4, in which f is fixed to zero, the optimum condition to raise T_c, and d is tentatively taken as 4.0 Å. From this exploration, we find that the most important parameter to enhance T_c is m^*. In particular, we need m^* larger than at least $2m_e$ to obtain T_c over 10 K, irrespective of any choice of other parameters, and T_c is optimized for m^* in the range $(10–20)m_e$. The optimized T_c depends rather strongly on the parameters to control the polar-coupling strength such as Z and the atomic mass A; if we choose a trivalent light atom such as boron to make $\omega_t(0)$ large, the optimum T_c is about 100 K, but the problem about the light atoms is that m^* will never become heavy due to the absence of either d or f electrons. Therefore, we do not expect that T_c would become much larger than

10 K, even if BeC_2 or BC_2 were synthesized. From this perspective, it will be much better to intercalate Ti or V, rather than Be or B. Taking all these points into account, we suggest synthesizing three-element GICs providing a heavy 3D electron system by the introduction of heavy atoms into a light-atom polar-crystal environment.

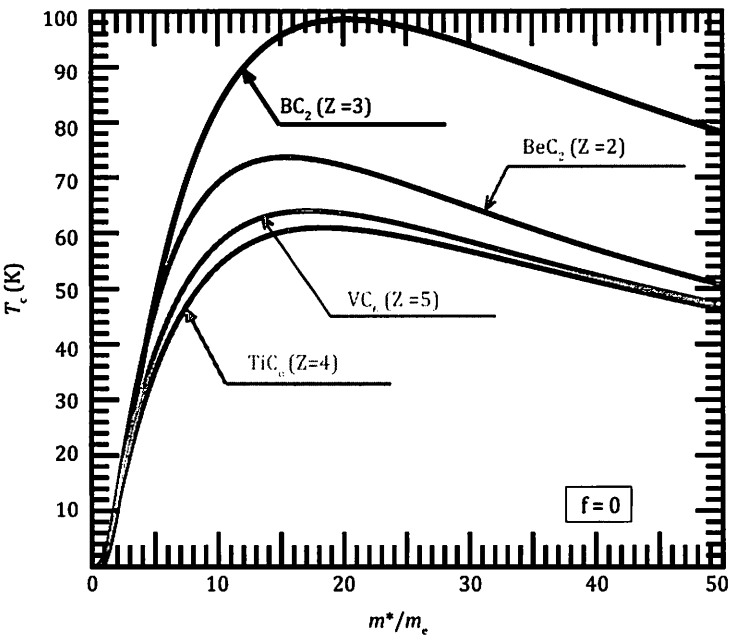

Figure 8.4 Prediction of T_c as a function of m^* for various GICs in pursuit of optimum T_c. We assume the fractional factor $f = 0$.

8.4 Strong-Coupling Approach with Application to Fullerides

8.4.1 Coherence Length

In the BCS theory for superconductivity which is applicable to superconductors in the weak-coupling region, T_c is directly related to the coherence length ξ_0 which characterizes the spatial extent of the wave function representing the bound state of a Cooper pair at zero temperature. More concretely, the relation between them is expressed as $T_c/E_F = 2e^{\gamma}/\pi^2(p_F\xi_0)^{-1} \approx 0.361/p_F\xi_0$ with

$\gamma(=0.57721\cdots)$ the Euler–Mascheroni constant and p_F the Fermi wave number. Because p_F^{-1} is in proportion to the lattice constant a_0, the relation is rewritten into the form as

$$\frac{T_c}{E_F} \approx 0.0735 \frac{a_0}{\xi_0} \tag{8.16}$$

for a monovalent metal in the fcc lattice structure. (For other valence and/or crystal structure, the coefficient of 0.0735 changes, but it always remains in the same order of magnitude.) For usual elemental superconductors, T_c/E_F is of the order of 10^{-4} and thus ξ_0 is about a thousand times larger than a_0, validating the approach in momentum space. On the other hand, the relation in Eq. (8.16) implies that high T_c is inevitably associated with short ξ_0. In fact, ξ_0 is observed as only a few nm or less, i.e., of the same order of a_0 in many of the recently synthesized high-T_c superconductors [see, e.g., Ref. 76] such as the cuprates, the alkali-doped C_{60}, and MgB_2.

A similar message can be obtained through the so-called Uemura plot [77–79], according to which there is a universal relation of $T_c/E_F \approx 0.04$ for a wide variety of strong-coupling superconductors. If this relation is put into Eq. (8.16), we obtain $\xi_0 \approx 2a_0$. Furthermore, if we think of the Bose–Einstein condensation (BEC) for an assembly of very tightly bound pairs of electrons, the condensation temperature (which amounts to T_c in such a system) is given by $T_c/E_F = (2/9\pi\zeta(3/2)^2)^{1/3} \approx 0.218$, where $\zeta(3/2)(=2.6124\cdots)$ is the Riemann's zeta function $\zeta(x)$ at $x = 3/2$. This value of T_c/E_F (which must be the optimum value for fermionic superconductors) suggests $\xi_0 \approx 0.3\, a_0$. Thus, in treating superconductivity in the strong-coupling region, we need to consider a situation of extremely short ξ_0, validating the approach in real space, which is totally different from that of very long ξ_0 in the weak-coupling superconductors.

8.4.2 Pairing Interaction in the Strong-Coupling Region

In view of the above-mentioned difference in ξ_0, we shall exploit the shortness of ξ_0 in reformulating the problem of making a quantitative calculation of T_c for strong-coupling superconductors in the Green's function approach [26]. Let us start with this

reformulation by considering the dynamical correlation function for singlet pairing of two electrons in the normal state $Q_{sc}^{R}(\mathbf{q},\omega)$, which is defined as

$$Q_{sc}^{R}(\mathbf{q},\omega) = -i\int_0^\infty dt\, e^{i\omega t - \eta t} \left\langle [e^{iHt}\Phi_{\mathbf{q}} e^{-iHt}, \Phi_{\mathbf{q}}^{+}] \right\rangle, \tag{8.17}$$

where H is the Hamiltonian for a homogeneous electron system and $\Phi_{\mathbf{q}}$ is the electron-pair annihilation operator, defined by $\Phi_{\mathbf{q}} \equiv \sum_{\mathbf{p}} c_{\mathbf{p}+\mathbf{q}\uparrow} c_{-\mathbf{p}\downarrow}$. In terms of the retarded pairing correlation function $Q_{sc}^{R}(\mathbf{q},\omega)$, we can define T_c as the temperature at which $Q_{sc}^{R}(\mathbf{q},\omega)$ diverges at $\mathbf{q}=0$ in the static limit ($\omega \to 0$) with the decrease of T.

As shown schematically in Fig. 8.5(a), Q_{sc} is conventionally divided into a sum of terms classified by the number of $\tilde{J}$s, where $\tilde{J}$, which has already appeared in Eq. (8.4), is the irreducible electron–electron effective interaction including all vertex corrections. Using $\Pi_{sc}(\mathbf{q}, \omega)$ the pairing polarization function composed of two *full* electron Green's functions including all self-energy corrections, we can express the infinite sum in Fig. 8.5(a) in a quite symbolical way as

$$Q_{sc} = -\frac{\Pi_{sc}}{1+\tilde{J}\Pi_{sc}}. \tag{8.18}$$

Then, the divergence in $Q_{sc}^{R}(0,\omega \to 0)$ occurs at the zero of the denominator in Eq. (8.18), which provides exactly the same T_c as that obtained through the solution of Eq. (8.4).

Now, instead of using Π_{sc}, we shall consider an alternative expansion with use of $\Pi_{sc,0}$ the pairing polarization function composed of two *bare* electron Green's functions. As shown schematically in Fig. 8.5(b), if we introduce the pairing interaction $\tilde{g}$ by the definition of

$$\tilde{g} \equiv \tilde{J} + \frac{1}{\Pi_{sc}} - \frac{1}{\Pi_{sc,0}}, \tag{8.19}$$

we can rewrite Q_{sc} in Eq. (8.18) into another exact form as

$$Q_{sc} = -\frac{\Pi_{sc,0}}{1+\tilde{g}\Pi_{sc,0}}. \tag{8.20}$$

Since we can always calculate $\Pi_{sc,0}$ easily, the problem of estimating T_c is reduced to the evaluation of $\tilde{g}$ in the limit of $\omega \to 0$ at $\mathbf{q} = 0$. Note that $\tilde{g}$ does not depend strongly on either $\mathbf{q}$ or ω, in sharp contrast with $\Pi^{R}_{sc,0}(\mathbf{q},\omega)$. In the BCS theory, for example, $\tilde{g}$ is taken as a constant which represents a weakly attractive and spatially local interaction working only in the vicinity of the Fermi level, given that the phonon energy ω_0 is much smaller than E_F. Then the zero of the denominator in Eq. (8.20) at $\mathbf{q} = 0$ and $\omega \to 0$ provides the well-known BCS formula for T_c. Note also that the problem of finding the zero of $1+\tilde{g}\Pi^{R}_{sc,0}(0,\omega\to 0)$ is just the same as that of solving the gap equation in Eq. (8.6) with replacing $V(\mathbf{p}-\mathbf{p}', i\omega_p - i\omega_{p'})$ by $\tilde{g}$.

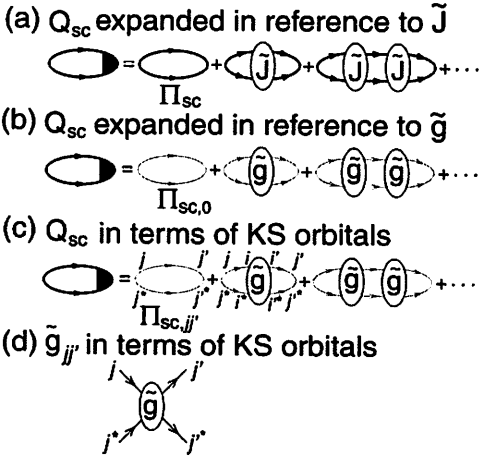

Figure 8.5 Pair correlation function Q_{sc} described in terms of using either (a) the pairing polarization function Π_{sc} and the irreducible electron–electron effective interaction $\tilde{J}$ or (b) the non-interacting pairing polarization function $\Pi_{sc,0}$ and the effective interaction $\tilde{g}$. By the extension of the idea of expanding Q_{sc} with use of $\Pi_{sc,0}$, we show a scheme to express it in terms of KS orbitals in (c), together with the schematic representation of $\tilde{g}_{jj'}$ in (d).

In the case of short ξ_0, we may assume that the essential physics of electron pairing can be captured even if we treat only a small-cluster system, as long as the system size is large enough in comparison with ξ_0. Under this assumption, we can take the following procedure for determining $\tilde{g}$: First, by representing the values for $\Pi_{sc,0}$ and $\tilde{g}$

in an N-site system as $\Pi_{sc,0}^{(N)}$ and $\tilde{g}_N$, respectively, we may write the pairing correlation function for the N-site system $Q_{sc}^{(N)}$ as

$$Q_{sc}^{(N)} = -\frac{\Pi_{sc,0}^{(N)}}{1+\tilde{g}_N \Pi_{sc,0}^{(N)}}, \tag{8.21}$$

in accordance with Eq. (8.20). In general, the exact bulk value $\tilde{g}$ will be obtained by taking the large-N limit of $\tilde{g}_N$, but expecting that $\tilde{g}_{N_0}$ with a small positive integer N_0 (for example, $N_0 \approx 2$) is already close to $\tilde{g}$, we may estimate $\tilde{g}$ by the relation of

$$\tilde{g} = -\frac{1}{Q_{sc,0}^{(N_0)}} - \frac{1}{\Pi_{sc,0}^{(N_0)}}, \tag{8.22}$$

with $Q_{sc}^{(N_0)}$ evaluated rigorously, for example, by exact diagonalization. Of course, we can determine a better value of $\tilde{g}$ by checking the saturation behavior of $\{\tilde{g}_{N_0}\}$ with the increase of N_0.

8.4.3 Interpolation Formula for the Pairing-Interaction Functional

Based on the knowledge so far obtained, let us speculate an appropriate functional form for the pairing interaction $K_{jj'}$ in SCDFT. It would be natural to expand the electron field operator in terms of the KS orbitals $\{|j\rangle\}$ in an inhomogeneous electron system, so that we can define the electron-pair operator Φ_j as $\Phi_j \equiv c_j c_{j^*}$ with $|j^*\rangle$ the time-reversed orbital of $|j\rangle$. Then, we can introduce the pairing polarization function in terms of Φ_j and $\Phi_j^\dagger$. In particular, we can calculate this quantity in the non-interactiong system $\Pi_{sc,jj'}$ in analogy with $\Pi_{sc,0}$, as schematically introduced in Fig. 8.5(c). At the same time, we can define a quantity $\tilde{g}_{jj'}$ as schematically shown in Fig. 8.5(d).

In the strong-coupling region, we do not expect that this $\tilde{g}_{jj'}$ exhibits strong dependence on $i\Omega$, because the Fermi energy, the scale for the electron kinetic energy, must be much smaller than the energy scale representing electron–electron interactions. In addition, $\tilde{g}_{jj'}$ does not depend strongly on orbital variables, either, because the pairing interaction should be short-ranged in real space in line with the shortness of ξ_0. Thus, we may regard $\tilde{g}_{jj'}$ as a constant. Then, if

we take $K_{jj'}$ in Eq. (8.1) as $\tilde{g}_{jj'}$, we can easily see that both Eq. (8.1) and the zero of $1+\tilde{g}_{jj'}\Pi^{R}_{sc,jj'}$ provide the same T_c.

In a more general situation of the intermediate-coupling region, however, $\tilde{g}_{jj'}$ will depend on both $i\Omega$ and orbital variables. In order to treat such a situation and also by paying attention to the weak-coupling situation examined in the previous section, we propose the functional form for $K_{jj'}$ in exactly the same form as that in Eq. (8.11) with replacing $V_{jj'}(i\Omega)$ by $\tilde{g}_{jj'}(i\Omega)$. Note that this functional form of $K_{jj'}$ is reduced to $\tilde{g}_{jj'}(0)$, if $\tilde{g}_{jj'}(i\Omega)$ does not depend on Ω, assuring us that the framework in SCDFT with this choice of $K_{jj'}$ provides the same T_c as that in the usual Green's function approach in the strong-coupling region. This means that we can successfully take care of both self-energy and vertex corrections beyond the G_0W_0 approximation by upgrading $V_{jj'}(i\Omega)$ to $\tilde{g}_{jj'}(i\Omega)$ in Eq. (8.11).

8.4.4 Alkali-Doped Fullerides

8.4.4.1 Aims of this subsection

The fulleride is a molecular crystal with narrow threefold conduction bands (with the band width $W \approx 0.5$ eV) derived from the t_{1u} electronic levels of each C_{60} molecule. With the doping of three alkali atoms per one C_{60} molecule, we obtain the half-filled situation in which superconductivity occurs with T_c in the range 18–38 K [15,16] and the short coherence length ξ_0 of only a few molecular units. As for the mechanism of superconductivity in the alkali-doped fullerides, phonons are widely believed to play an important role. This belief is based upon a crude estimate of T_c in the conventional Eliashberg theory. In fact, analysis of various experiments with use of this theory has shown that many aspects of superconductivity in these fullerides are consistent with a picture of s-wave BCS superconductors with the Cooper pairs driven by the coupling to the intramolecular high-frequency phonons in H_g symmetry (with the phonon energy $\omega_0 \approx$ 0.2 eV and the non-dimensional electron–phonon coupling constant $\lambda \approx 0.6$ for Rb_3C_{60}) [17,80,81].

The above picture, however, seems to be too much simplified and we may raise several fundamental questions. From a theoretical point of view, one of the serious problems is ill foundation to adopt

the Eliashberg theory in the fullerides due to the importance of vertex corrections [19,82]. From an experimental side, the following four experimental facts have been observed which we cannot easily understand with use of the Eliashberg theory: (i) The relation between T_c and the lattice constant a_0 changes remarkably when the crystal structure changes from the face-centered cubic (fcc) to simple cubic (sc) lattice by the introduction of Na, a smaller ion compared to K, Rb, or Cs, as a dopant ion [83]. (ii) The antiferromagnetic (AF) insulating behavior has been reported in ammoniated K_3C_{60}, which is peculiar in the sense that s-wave BCS superconductivity exists in the vicinity of an AF phase [84]. A similar problem is also seen in the body-centered cubic A15-structured Cs_3C_{60} [16]. (iii) The anomalous ^{13}C isotope effect on T_c for 50% ^{13}C substitution has been observed, reflecting the difference between the molecular and atomic mixture of ^{12}C and ^{13}C atoms [85]. (iv) With the deviation of electron number per site n from half-filling, T_c decreases rapidly in both sides of the deviation [86].

Although the experiment (i) may be reproduced in the Eliashberg theory with some judicious choice of parameters, the rest (ii–iv) cannot be explained even qualitatively in the theory. In addition, the behavior of T_c as a function of n observed in the experiment (iv) cannot be predicted either by those theories proposed so far to account for the copper oxide high-T_c superconductivity based on some strong-correlation models, though such models may be favorable for the explanation of the experiment (ii).

A successful theory for the fullerene superconductors should not only reproduce these experiments in a coherent fashion but also clarify the reason why the effect of vertex corrections, even if it is large, does not manifest itself in many superconducting properties. In quest of such a theory from a somewhat general viewpoint, the present author made intensive studies of the Hubbard–Holstein (HH) model and its extension in the past and successfully explained all the issues (i–iv) raised above [18,87–91]. In the rest of this subsection, we shall focus on the first three issues in order to show how nicely the HH model applies to the fullerides, as far as T_c is concerned. Then we shall explore a possibility to enhance T_c in this class of superconductors by changing the parameters involved in the model.

8.4.4.2 The Hubbard–Holstein model

In a molecular crystal, it is a very good approximation to regard each molecular unit as a "site" in a lattice. We shall adopt this approximation and describe the electron–phonon system in the alkali-doped fullerides by a model Hamiltonian H in site representation in which each site corresponds to each C_{60} molecular unit. Since the conduction band width is narrow, the intermolecular hopping integral t must be small, indicating that only the nearest-neighbor hopping is relevant in modeling the kinetic energy of the system. Then, it would be appropriate to decompose H into the nearest-neighbor electron-transfer term H_t and the sum of site terms $\sum_i H_i$ including both the electron–electron and the electron–local phonon interactions. In order to faithfully represent the threefold degenerate t_{1u}-conduction bands coupled with eight H_g intramolecular Jahn–Teller (JT) phonons, we would need to include the $t_{1u} \otimes H_g$ JT structure in H_i, as has often been the case [92–95]. In making a detailed study on the stability of the AF insulating phase, it is known that this feature of band multiplicity plays a rather crucial role [96], but in treating superconductivity itself, the band multiplicity is not considered to be of primary importance [97]. Therefore, we shall take a simplest possible model, namely, the *one-band* HH model to discuss superconductivity from a more general viewpoint that will be applicable to the whole family of fullerene superconductors including not only electron-doped but also hole-doped materials with different JT structures.

The concrete form for H in the HH model is given by

$$H = -t \sum_{\langle i,i' \rangle \sigma} (c_{i\sigma}^{\dagger} c_{i'\sigma} + \text{h.c.}) + \sum_i H_i, \tag{8.23}$$

with the site term H_i written as

$$H_i = -\mu \sum_{\sigma} n_{i\sigma} + U n_{i\uparrow} n_{i\downarrow} + \sqrt{\alpha}\omega_0 \sum_{\sigma} n_{i\sigma}(a_i + a_i^{\dagger}) + \omega_0 a_i^{\dagger} a_i, \tag{8.24}$$

where $\langle i,i' \rangle$ represents the nearest-neighbor-site pair, $c_{i\sigma}$ the operator to annihilate a spin-σ electron at site i, μ the chemical potential, $n_{i\sigma} \equiv c_{i\sigma}^{\dagger} c_{i\sigma}$, U the on-site (or intramolecular) Coulomb repulsion, α the nondimensional electron–phonon coupling constant which is related to the conventional electron–phonon coupling constant

λ through $\lambda = \alpha\omega_0/tz$ with ω_0 the optical-phonon energy and z the coordination number, and a_i the operator to annihilate an optical phonon at site i.

The characteristic features of the fullerenes can be well captured by an appropriate choice of the parameters involved in this Hamiltonian. In fact, the narrowness of the conduction band can be described by the smallness of t of the order of 0.1 eV. The difference in the crystal structure as well as the effect of band multiplicity can be well accounted for by a suitable choice of z. The high-frequency intramolecular optical phonons coupled strongly to electrons can be treated by considering the local phonons with the energy ω_0($\approx$0.2 eV) at each site. The short-range Coulomb potential must be relevant in the fullerenes due to the proximity to the AF state and it can be included by the introduction of U. Note that this U is not the direct Coulomb repulsion between electrons on a carbon atom U_{atom} which is of the order of 5–10 eV. Rather it is the sum of U_{atom} and the attraction $-U_{\text{pol}}$ due to the electronic polarization effect of 60 π-electrons in the C_{60} molecule [98]. Because of a strong cancellation between U_{atom} and $-U_{\text{pol}}$, U is expected to be of the order of 0.1 eV, which is about the same magnitude as that for the phonon-mediated attraction, $-U_{\text{ph}} \equiv -2\alpha\omega_0$.

Intensive studies on the ground state in this system by exact diagonalization of small-size clusters have revealed that the half-filled HH model exhibits interesting competition among charge-density-wave (CDW), spin-density-wave (SDW), and superconducting states [88,90]. We may summarize the results in the following way: (a) If U–U_{ph} is at least smaller than $-t$, the CDW state composed of an array of immobile bipolarons is stabilized. (b) If U–U_{ph} is larger than t, there appears the SDW state which is nothing but the AF state in this case. (c) Superconductivity appears only in the CDW–SDW transition region where $|U\text{–}U_{\text{ph}}|$ is less than t. In this offset situation of $U \approx U_{\text{ph}}$, the state may be regarded as an assembly of nearly free polarons and the main effect of the strong electron–phonon vertex corrections is found to form a polaron from a bare electron. This implies that the Eliashberg theory or even the BCS theory is expected to be accurate enough to describe superconductivity in this system, if it is applied on the basis of the polaron picture [88,90,99]. In any case, the intrinsic competition of superconductivity with the AF state in the half-filled HH model resolves the issue (ii) raised previously.

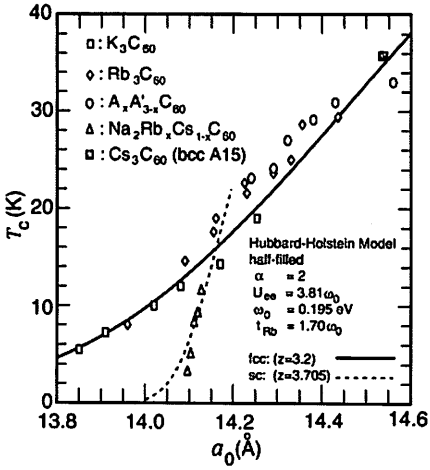

Figure 8.6 T_c as a function of the lattice constant a_0 in the alkali-doped fullerides and its dependence on the crystal structure. The solid and the broken curves represent our theoretical results, while the experimental results are given by square, triangle, diamond, and circle marks.

In order to address the issue (i), we have applied our framework to calculate T_c to the HH model by estimating $\tilde{g}$ with use of a cluster as small as two molecules (i.e., $N_0 = 2$). We have evaluated the variation of t with the change of the lattice constant a_0 by fitting the change in the band width obtained by the band-structure calculation for each lattice structure [100,101]. More specifically, t is determined by

$$t = t_{Rb} \frac{d}{d_{Rb}} \exp\left(-\frac{d - d_{Rb}}{\Delta} \right), \tag{8.25}$$

with $d = a_0/\sqrt{2} - 6.95$ Å, Δ = 0.55 Å, and the corresponding parameters, t_{Rb} and d_{Rb}, for Rb_3C_{60}. By choosing $t_{Rb} = 1.70\omega_0$ suitable for Rb_3C_{60} and the common parameters such as $U = 3.81\omega_0$, $\alpha = 2$, and ω_0 = 0.195 eV with reference to band-structure calculations and relevant experiments, we obtain the results for T_c as a function of a_0, which agrees remarkably well with experiment as clearly demonstrated in Fig. 8.6. Note that in our calculation, the difference in T_c between fcc and sc structures arises mainly from that in the "effective" lattice coordination number z [81]. This indicates that z is a key to the resolution of the issue (i). Note also that the recent experimental result for Cs_3C_{60} under pressure is also on

our theoretical curve, if we estimate an appropriate value of a_0 so as to reproduce the same volume per one C_{60} molecule for this bcc A15 structure.

The competing feature between U_{ph} and U is also identified to be a key to the resolution of the issue (iii) [89]. The observed anomalous isotope effect cannot be explained by either the phonon or the electronic polarization mechanism alone. It can be reproduced, if both these mechanisms are included simultaneously. Namely, we need to consider the change in both ω_0 and U induced by the isotope substitution. The sensitivity of T_c to the local change in the Coulomb potential U is due to the very short-range nature of ξ_0 of this superconductivity.

8.4.4.3 Prospect for room-temperature superconductors

Encouraged by the success in reproducing T_c for the alkali-doped fullerene superconductors by the application of our theoretical framework to the HH model at half-filling in the nearly offset situation of $U \approx U_{ph}$, we have attempted to explore the optimum value of T_c with the increase of the electron–phonon coupling constant α, whereby U is also increased to keep the offset situation. Examples of the calculated results of T_c are plotted in Fig. 8.7. As is seen, T_c goes beyond 100 K for $\alpha = 3$ and it reaches room temperature for $\alpha = 4$.

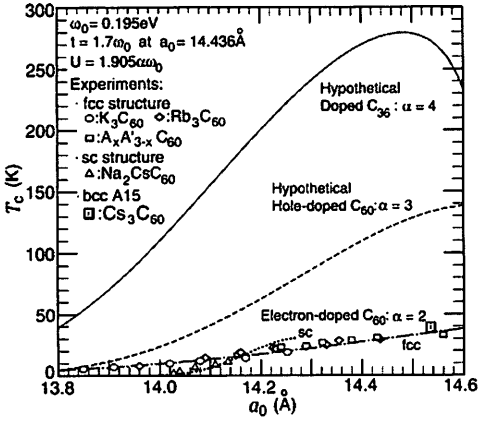

Figure 8.7 T_c as a function of the lattice constant a_0. For electron-doped C_{60} with $\alpha = 2$, the theoretical curves are drawn, together with the experimental results. We also give the results for both $\alpha = 3$ and 4 corresponding to (hypothetical) hole-doped C_{60} and doped C_{36}.

By the band-structure calculation [102], it is known that α is about three for the hole-doped C_{60} in which hole carriers will be introduced into the h_u-valence bands. On the other hand, in the crystal composed of C_{36}, α will be about four [103], if the C_{36} solid is successfully doped to have an enough number of mobile carriers in the system, although it seems to be a very difficult task [104].

8.5 Conclusion and Discussion

In this chapter, we have proposed a new functional form for the pairing interaction $K_{jj'}$, a key quantity in the gap equation, Eq. (8.1), to determine T_c in the DFT for superconductors. The functional form is given in Eq. (8.11) with the effective electron electron interaction $V_{jj'}(i\Omega)$ replaced by $\tilde{g}_{jj'}(i\Omega)$ defined schematically in Fig. 8.5(d). We have assessed the usefulness of this functional form by its applications to both the weak-coupling superconductors like the alkali- and alkaline-earth-intercalated graphites and the strong-coupling superconductors like the alkali-doped fullerides. We have also explored a possibility to enhance T_c up to room temperature.

The proposed functional form has just opened a challenging frontier of the research on high-T_c superconductivity. Although we need to improve on the functional form itself by utilizing the information obtained by its application to a much wider range of materials, we can think of several ways to make use of this new theoretical tool. For example, we can make a quantitative assessment of the effectiveness of each superconducting mechanism, either phononic or electronic, so far proposed by investigating how much T_c is actually enhanced with the introduction of the mechanism. The knowledge accumulated by such investigations will pave the way to reach a room-temperature superconductor.

Acknowledgments

This work is supported by a Grant-in-Aid for Scientific Research (C) (No. 21540353) from MEXT, Japan.

References

1. W.L. McMillan, *Phys. Rev.* **167**, 331 (1968).
2. P.B. Allen, R.C. Dynes, *Phys. Rev.* B **12**, 905 (1975).
3. P.B. Allen, B. Mitrović, in *Solid State Physics,* edited by H. Ehrenreich, F. Seitz, D. Turnbull, Vol. **37** p. 1. (Academic, New York, 1982).
4. J.P. Carbotte, *Rev. Mod. Phys.* **62**, 1027 1990.
5. G.M. Eliashberg, *Sov. Phys.-JETP* **11**, 696 (1960).
6. P. Morel, P.W. Anderson, *Phys. Rev.* **125**, 1263 (1962).
7. K.-P. Bohnen, R. Heid, B. Renker, *Phys. Rev. Lett.* **86**, 5771 (2001).
8. Y. Kong, O.V. Dolgov, O. Jepsen, O.K. Andersen, *Phys. Rev.* B **64**, 020501(R) (2001).
9. H.J. Choi, D. Roundy, H. Sun, M.L. Cohen, S.G. Louie, *Nature* **418**, 758 (2002).
10. H.J. Choi, D. Roundy, H. Sun, M.L. Cohen, S.G. Louie, *Phys. Rev.* B **66**, 020513(R) (2002).
11. I.I. Mazin, *Phys. Rev. Lett.* **95**, 227001 (2005).
12. M. Calandra, F. Mauri, *Phys. Rev. Lett.* **95**, 237002 (2005).
13. Y. Takada, *J. Phys. Soc. Jpn.* **45**, 786 (1978).
14. Y. Takada, *Phys. Rev.* B **47**, 5202 (1993).
15. A.F. Hebard, M.J. Rosseinsky, R.C. Haddon, et al, *Nature* **350**, 600 (1991).
16. Y. Takabayashi, A.Y. Ganin, P. Jeglič, et al, *Science* **323**, 1585 (2009).
17. O. Gunnarsson, *Rev. Mod. Phys.* **69**, 575 (1997).
18. Y. Takada, T. Hotta, *Int. J. Mod. Phys.* B **12**, 3042 (1998).
19. Y. Takada, *J. Phys. Chem. Solids* **54**, 1779 (1993).
20. Y. Takada, *Phys. Rev.* B **52**, 12708 (1995).
21. Y. Takada, *Phys. Rev. Lett.* **87**, 226402 (2001).
22. L.N. Oliveira, E.K.U. Gross, W. Kohn, *Phys. Rev. Lett.* **60**, 2430 (1988).
23. S. Kurth, M. Marques, M. Lüders, E.K.U. Gross, *Phys. Rev. Lett.* **83**, 2628 (1999).
24. Y. Takada, *J. Phys. Soc. Jpn.* **78**, 013703 (2009).
25. Y. Takada, *J. Supercond. Nov. Magn.* **22**, 89 (2009).
26. Y. Takada, *Int. J. Mod. Phys.* B **21**, 3138 (2007).
27. P. Hohenberg, W. Kohn, *Phys. Rev.* **136**, 864 (1964).
28. W. Kohn, L.J. Sham, *Phys. Rev.* **140**, A1133 (1965).

29. P.G. de Gennes, *Superconductivity of Metals and Alloys*, (Benjamin, New York, 1966).
30. J.P. Perdew, M. Levy, *Phys. Rev. Lett.* **51**, 1884 (1983).
31. L.J. Sham, M. Schlüter, *Phys. Rev. Lett.* **51**, 1888 (1983).
32. L.J. Sham, M. Schlüter, *Phys. Rev.* B **32**, 3883 (1985).
33. M. Lüders, M.A.L. Marques, N.N. Lathiotakis, et al, *Phys. Rev.* B **72**, 024545 (2005).
34. A. Sanna, G. Profeta, A. Floris, A. Marini, E.K.U. Gross, S. Massidda, *Phys. Rev.* B **75**, 020511(R) (2007).
35. M.A.L. Marques, M. Lüders, N.N. Lathiotakis, et al, *Phys. Rev.* B **72**, 024546 (2005).
36. A. Floris, G. Profeta, N.N. Lathiotakis, et al, *Phys. Rev. Lett.* **94**, 037004 (2005).
37. G. Profeta, C. Franchini, N.N. Lathiotakis, et al, *Phys. Rev. Lett.* **96**, 047003 (2006).
38. A. Sanna, C. Franchini, A. Floris, et al, *Phys. Rev.* B **73**, 144512 (2006).
39. A. Floris, A. Sanna, S. Massidda, E.K.U. Gross, *Phys. Rev.* B **75**, 054508 (2007).
40. J.P. Perdew, K. Burke, M. Ernzerhof, *Phys. Rev. Lett.* **77**, 3865 (1996); *ibid.* **78**, 1396 (1997) (E).
41. M.L. Cohen, *Phys. Rev.* **134**, *A* 511 (1964).
42. M.L. Cohen, in "Superconductivity" e.d. R.D. Parks (Marcel Dekker, New York, 1969) Vol. 1, Chap. 12.
43. Y. Takada, *J. Phys. Soc. Jpn.* **49**, 1267 (1980).
44. D.A. Kirzhnits, E.G. Maksimov, D.I. Khomskii, *J. Low Temp. Phys.* **10**, 79 (1973).
45. C.S. Koonce, M.L. Cohen, J.F. Schooley, W.R. Hosler, E.R. Pfeiffer, *Phys. Rev.* **163**, 380 (1967).
46. X. Lin, Z. Zhu, B. Fauquè, K. Behnia, *Phys. Rev. X* **3**, 021002 (2013).
47. J.E. Fischer, T.E. Thompson, *Phys. Today* **31**, 36(7) (1978).
48. H. Kamimura, *Phys. Today* **40**, 64(12) (1987).
49. H. Zabel, S.A. Solin (eds.), *Graphite Intercalation Compounds II*, Springer-Verlag, 1992.
50. M.S. Dresselhaus, G. Dresselhaus, *Adv. Phys.* **51**, 1 (2002).
51. N.B. Hannay, T.H. Geballe, B.T. Matthias, K. Andres, P. Schmidt, D. MacNair, *Phys. Rev. Lett.* **14**, 225 (1965).

52. Y. Koike, H. Suematsu, K. Higuchi, S. Tanuma, *Solid State Commun.* **27**, 623 (1978).
53. M. Kobayashi, I. Tsujikawa, *J. Phys. Soc. Jpn.* **46**, 1945 (1979).
54. Y. Koike, H. Suematsu, K. Higuchi, S. Tanuma, *Physica* B **99**, 503 (1980).
55. M.G. Alexander, D.P. Goshorn, D. Guerard, P. Lagrange, M. El Makrini, D.G. Onn, *Synth. Met.* **2**, 203 (1980).
56. Y. Iye, S. Tanuma, *Phys. Rev.* B **25**, 4583 (1982).
57. I.T. Belash, O.V. Zharikov, A.V. Pal'nichenko, *Synth. Met.* **34**, 455 (1989).
58. M.S. Dresselhaus, A. Chaiken, G. Dresselhaus, *Synth. Met.* **34**, 449 (1989).
59. I.T. Belash, A. D. Bronnikov, O.V. Zharikov, A.V. Pal'nichenko, *Synth. Met.* **36**, 283 (1990).
60. I.T. Belash, A. D. Bronnikov, O.V. Zharikov, A.V. Pal'nichenko, *Solid State Commun.* **69**, 921 (1989).
61. T.E. Weller, M. Ellerby, A.S. Saxena, R.P. Smith, N.T. Skipper, *Nature Phys.* **1**, 39 (2005).
62. N. Emery, C. Heérold, M. d'Astuto, et al, *Phys. Rev. Lett.* **95**, 087003 (2005).
63. A. Gauzzi, S. Takashima, N. Takeshita, et al, *Phys. Rev. Lett.* **98**, 067002 (2007).
64. J.S. Kim, L. Boeri, J.R. O'Brien, F.S. Razavi, R.K. Kremer, *Phys. Rev. Lett.* **99**, 027001 (2007).
65. J.S. Kim, R.K. Kremer, L. Boeri, F.S. Razavi, *Phys. Rev. Lett.* **96**, 217002 (2006).
66. C. Kurter, L. Ozyuzer, D. Mazur, et al, *Phys. Rev.* B **76**, 220502 (2007).
67. G. Csanyi, P.B. Littlewood, A.H. Nevidomskyy, C.J. Pickard, B.D. Simons, *Nature Phys.* **1**, 42 (2005).
68. D.G. Hinks, D. Rosenmann, H. Claus, M.S. Bailey, J.D. Jorgensen, *Phys. Rev.* B **75**, 014509 (2007).
69. M. Posternak, A. Baldereschi, A.J. Freeman, E. Wimmer, *Phys. Rev. Lett.* **52**, 863 (1984).
70. N.A.W. Holzwarth, S.G. Louie, S. Rabii, *Phys. Rev.* B **30**, 2219 (1984).
71. A. Koma, K. Miki, H. Suematsu, T. Ohno, H. Kamimura, *Phys. Rev.* B **34**, 2434 (1986).
72. T. Ohno, K. Nakao, H. Kamimura, *J. Phys. Soc. Jpn.* **47**, 1125 (1979).
73. G. Wang, W.R. Datars, P.K. Ummat, *Phys. Rev.* B **44**, 8294 (1991).
74. Y. Takada, *J. Phys. Soc. Jpn.* **51**, 63 (1982).
75. U. Mizutani, T. Kondow, T.B. Massalski, *Phys. Rev.* B **17**, 3165 (1978).

76. C.P. Poole, Jr., *Handbook of Superconductivity*, (Academic, San Diego, 2000).
77. Y.J. Uemura, L.P. Le, G.M. Luke, et al, *Phys. Rev. Lett.* **66**, 2665 (1991).
78. Y.J. Uemura, A. Keren, L.P. Le, et al, *Nature* **352**, 605 (1991).
79. Y. Takada, *J. Phys. Soc. Jpn.* **61**, 3849 (1992).
80. A.P. Ramirez, *Supercond. Rev.* **1**, 1 (1994).
81. M.P. Gelfand, *Supercond. Rev.* **1**, 103 (1994).
82. L. Pietronero, *Europhys. Lett.* **17**, 365 (1992).
83. K. Tanigaki, I. Hirosawa, T.W. Ebbesen, J. Mizuki, J.-S. Tsai, *J. Phys. Chem. Solids* **54**, 1645 (1993).
84. Y. Iwasa, H. Shimoda, T.T.M. Palstra, Y. Maniwa, O. Zhou, T. Mitani, *Phys. Rev.* B. **53**, R8836 (1996).
85. C. -C. Chen, C.M. Lieber, *Science* **259**, 655 (1993).
86. T. Yildirim, L. Barbedette, J.E. Fischer, et al, *Phys. Rev. Lett.* **77**, 167 (1996).
87. Y. Takada, T. Higuchi, *Phys. Rev.* B **52**, 12720 (1995).
88. Y. Takada, *J. Phys. Soc. Jpn.* **65**, 1544 (1996).
89. Y. Takada, *J. Phys. Soc. Jpn.* **65**, 3134 (1996).
90. T. Hotta, Y. Takada, *Physica* B **230–232** ,1037 (1997).
91. T. Hotta, Y. Takada, *Phys. Rev.* B **56**, 13916 (1997).
92. C.M. Varma, J. Zaanen, K. Raghavachari, *Science* **254**, 989 (1991).
93. A. Auerbach, N. Manini, E. Tosatti, *Phys. Rev.* B **49**, 12998 (1994).
94. A. Auerbach, N. Manini, E. Tosatti, *Phys. Rev.* B **49**, 13008 (1994).
95. J.E. Han, O. Gunnarsson, V.H. Crespi, *Phys. Rev. Lett.* **90**, 167006 (2003).
96. J.E. Han, E. Kock, O. Gunnarsson, *Phys. Rev. Lett.* **84**, 1276 (2000).
97. E. Cappelluti, P. Paci, C. Grimaldi, L. Pietronero, *Phys. Rev.* B **72**, 054521 (2005).
98. S. Chakravarty, M. Gelfand, S. Kivelson, *Science* **254**, 970 (1991).
99. A.S. Alexandrov, V.V. Kabanov, *Phys. Rev.* B **54**, 3655 (1996).
100. S. Satpathy, V.P. Antropov, O.K. Andersen, O. Jepsen, O. Gunnarsson, A.I. Liechtenstein, *Phys. Rev.* B **46**, 1773, (1992).
101. A. Oshiyama, S. Saito, *Solid State Commun.* **82**, 41 (1992).
102. I.I. Mazin, S.N. Rashkeev, V.P. Antropov, O. Jepsen, A.I. Lichtenstein, O.K. Andersen, *Phys. Rev.* B **45**, 5114 (1992).
103. M. Côté, J.C. Grossman, M.L. Cohen, S.G. Louie, *Phys. Rev. Lett.* **81**, 697 (1998).
104. C. Piskoti, J. Yarger, A. Zettl, *Nature* **393**, 771 (1998).

Index